Ligand Effects in C−H and C−C Bond Activation by Gas-Phase Transition Metal−Ligand Complexes

Brenda L. Tjelta and P. B. Armentrout*

Contribution from the Department of Chemistry, University of Utah, Salt Lake City, Utah 84112

Received January 12, 1996[⊗]

Abstract: Guided ion beam mass spectrometry has been used to examine the kinetic energy dependence of reactions of FeL^+ (L = CO and H_2O) with methane and ethane. Carbon−hydrogen and carbon−carbon bond activation is observed, and there is no evidence for direct interaction of either ligand in the chemistry. Thresholds for these processes are measured and converted to the following LFe^+-CH_3 0 K bond dissociation energies (BDEs): $D_0[(CO)Fe^+-CH_3] = 1.30 \pm 0.05$ eV and $D_0[(H_2O)Fe^+-CH_3] = 1.95 \pm 0.10$ eV. Comparison of these values to the previously determined $D_0(Fe^+-CH_3) = 2.37 \pm 0.05$ eV and to $D_0(LFe^+-D)$ bond energies permits a quantitative assessment of the effects of ligation on σ-bond activation by metal complexes. Differences in the abilities of the two FeL^+ species to activate methane and ethane are compared to the behavior of the two complexes activating D_2. As in the D_2 case, σ bond activation of these alkanes by $Fe(H_2O)^+$ is more efficient than $Fe(CO)^+$ at low energies. This result is rationalized in terms of different electronic structures at the ligated metal ion centers. In addition, it is found that the *selectivity* of the reactions is affected by ligation, such that $Fe(CO)^+$ activates the C−H and C−C bonds of ethane with comparable efficiency, while $Fe(H_2O)^+$ prefers to activate the C−H bonds.

Introduction

The activation of C−H and C−C bonds of alkanes by gas-phase atomic transition metal ions has been studied intensely over the past decade.[1−5] One means of relating this chemistry to that found in homogeneous catalysis is to examine systematically how the reactivity of the metal center varies with ligation. Fewer studies of such effects have been performed although it has been demonstrated that the addition of a single ligand to the metal center can dramatically alter the reactivity.[2,6−10] In most cases, there is little quantitative thermodynamic information that has accompanied these studies (notable exceptions are refs 9 and 10) and the ligands typically participate directly in the reactions. In the present study, we examine how ancillary ligands (those not actively involved in the reaction) can affect C−H and C−C bond activation. By using guided ion beam methods, we are able to quantitatively assess both the kinetic and thermodynamic differences in the reactions.

In this work, we examine C−H and C−C bond activation in the simplest alkanes, methane and ethane at an ionic iron center. We have previously[11] characterized the state-specific chemistry of these molecules with Fe^+ in its $^6D(4s^13d^6)$ ground electronic state and $^4F(3d^7)$ first excited state, 0.23 eV higher in energy.[12] In the methane system, reactions form $FeH^+ + CH_3$ (the dominant product) and $FeCH_3^+ + H$. Recently, we have also shown that $FeCH_2^+ + H_2$ is formed, but needs to surpass an activation barrier in excess of the endothermicity of this channel.[13] In this system, the ^4F excited state was found to be about 30 times more reactive than the ^6D ground state. In the ethane system, the major products are $FeCH_3^+ + CH_3$ and $FeH^+ + C_2H_5$, with small amounts of $Fe(C_2H_4)^+ + H_2$ and $FeC_2H_5^+ + H$ observed. Here, the excited state is about 40 times more reactive than the ground state.

The present work examines the effects on this chemistry induced by ligation of Fe^+ with CO and H_2O. We have previously determined the thermodynamic properties of these FeL^+ complexes[14,15] and their electronic properties have been theoretically characterized.[16,17] Our collision-induced dissociation (CID) studies have determined that the bond dissociation energies (BDEs) relative to the $Fe^+(^6D)$ asymptote for the two complexes are essentially equal: $D_0(Fe^+-CO) = 1.36 \pm 0.08$ eV[14] and $D_0(Fe^+-H_2O) = 1.32 \pm 0.05$ eV.[15] Theory finds that the ground state of $Fe(CO)^+$ is $^4\Sigma^-$,[16] while that of $Fe(H_2O)^+$ is $^6A_1$,[17] and both metal−ligand interactions are calculated to be largely electrostatic in nature. Thus, the reactivities of these two complexes are expected to be different based on electronic but not thermodynamic considerations. Further, there is the possibility that CO can couple with the C−H and C−C bond cleavage products to form aldehyde, ketone, formyl, and acetyl

[⊗] Abstract published in *Advance ACS Abstracts,* October 1, 1996.

(1) Allison, J.; Freas, R. B.; Ridge, D. P. *J. Am. Chem. Soc.* **1979**, *101*, 1332.
(2) Eller, K.; Schwarz, H. *Chem. Rev.* **1991**, *91*, 1121.
(3) *Gas Phase Inorganic Chemistry*, Russell, D. H., Ed.; Plenum: New York, 1989.
(4) Armentrout, P. B. In *Selective Hydrocarbon Activation: Principles and Progress*; Davies, J. A., Watson, P. L., Liebman, J. F., Greenberg, A., Eds.; VCH: New York, 1990; pp 467−533.
(5) Weisshaar, J. C. *Adv. Chem. Phys.* **1992**, *82*, 213. Weisshaar, J. C. *Acc. Chem. Res.* **1993**, *26*, 213.
(6) Jacobson, D. B.; Freiser, B. S. *J. Am. Chem. Soc.* **1984**, *106*, 3891. Jackson, T. C.; Jacobson, D. B.; Freiser, B. S. *J. Am. Chem. Soc.* **1984**, *106*, 1252.
(7) Huang, S. K.; Allison, J. *Organometallics* **1983**, *2*, 833. Freas, R. B.; Ridge, D. P. *J. Am. Chem. Soc.* **1980**, *102*, 7129.
(8) Fiedler, A.; Schroder, D.; Shaik, S.; Schwarz, H. *J. Am. Chem. Soc.* **1994**, *116*, 10734. Ryan, M. F.; Fiedler, A.; Schroder, D.; Schwarz, H. *Organometallics* **1994**, *13*, 4072.
(9) Clemmer, D. E.; Aristov, N.; Armentrout, P. B. *J. Phys. Chem.* **1993**, *97*, 544. Clemmer, D. E.; Chen, Y.-M.; Khan, F. A.; Armentrout, P. B. *J. Phys. Chem.* **1994**, *98*, 6522. Chen, Y.-M.; Clemmer, D. E.; Armentrout, P. B. *J. Am. Chem. Soc.* **1994**, *116*, 7815.
(10) Bushnell, J. E.; Kemper, P. R.; Maitre, P.; Bowers, M. T. *J. Am. Chem. Soc.* **1994**, *116*, 9710. van Koppen, P. A. M.; Kemper, P. R.; Bushnell, J. E.; Bowers, M. T. *J. Am. Chem. Soc.* **1995**, *117*, 2098.
(11) Schultz, R. H.; Elkind, J. L.; Armentrout, P. B. *J. Am. Chem. Soc.* **1988**, *110*, 411.
(12) Sugar, J.; Corliss, C. *J. Chem. Phys. Ref. Data* **1985**, *14*, 1.
(13) Haynes, C. L.; Chen, Y.-M.; Armentrout, P. B. *J. Phys. Chem.* **1996**, *100*, 111.
(14) Schultz, R. H.; Crellin, K. C.; Armentrout, P. B. *J. Am. Chem. Soc.* **1991**, *113*, 8590.
(15) Schultz, R. H.; Armentrout, P. B. *J. Phys. Chem.* **1993**, *97*, 596.
(16) Barnes, L. A.; Rosi, M.; Bauschlicher, C. W., Jr. *J. Chem. Phys.* **1990**, *93*, 609.
(17) Rosi, M.; Bauschlicher, C. W., Jr. *J. Chem. Phys.* **1989**, *90*, 7264. Rosi, M.; Bauschlicher, C. W., Jr. *J. Chem. Phys.* **1990**, *92*, 1876.

S0002-7863(96)00104-7 CCC: $12.00

species, while no such coupling is anticipated for the H_2O ligand. Finally, we compare these results to those previously reported for the reactions of $Fe(CO)^+$ and $Fe(H_2O)^+$ with D_2.[18]

Experimental Section

The guided-ion beam instrument on which these experiments were performed has been described in detail previously.[19,20] Ions are created in a flow tube source as described below, extracted from the source, accelerated, and passed through a magnetic sector for mass analysis. The mass-selected ions are decelerated to the desired kinetic energy and focused into an octopole beam guide. This device uses radio-frequency electric fields to trap the ions in the radial direction to ensure complete collection of reactant and product ions.[21] The octopole passes through a gas cell that contains the neutral collision partner at a fairly low pressure. Studies performed at three different pressures (~0.05, 0.1, and 0.2 mTorr) demonstrated that none of the product cross sections exhibit any dependence on the pressure of the neutral reactant. The unreacted parent and product ions drift to the end of the octopole from which they are extracted, passed through a quadrupole mass filter for mass analysis, and detected with a secondary electron scintillation ion detector using standard pulse counting techniques. Raw ion intensities are converted to cross sections as described previously.[19] We estimate absolute cross sections to be accurate to ±20%.

Laboratory (lab) energies are converted to energies in the center of mass (CM) frame by using the conversion $E_{CM} = E_{lab}M/(M + m)$, where m and M are the ion and neutral masses, respectively. The absolute energy scale and corresponding full width at half maximum (fwhm) of the ion beam kinetic energy distribution are determined by using the octopole as a retarding energy analyzer as described previously.[19] The absolute uncertainty in the energy scale is ±0.05 eV (lab). The ion energy distributions are nearly Gaussian and have a typical fwhm of 0.2−0.5 eV (lab).

Ion Source. The metal−ligand ions are formed in a 1 m long flow tube[22] operating at a pressure of 0.4−0.7 Torr with a helium flow rate of 4000−9000 standard cm^3/min. Ions are produced by two methods. In the first method, He^+ and He* are formed in a microwave discharge and react further downstream with $Fe(CO)_5$ added to the flow. $Fe(CO)^+$ is produced directly, and $Fe(H_2O)^+$ can be produced by adding water vapor diluted by helium to the flow. In the second method, Fe^+ is produced by argon ion sputtering of an iron cathode in a flow of 5−10% argon in helium. $Fe(H_2O)^+$ and $Fe(CO)^+$ are formed by associative reactions of Fe^+ with the ligand molecules added 10 cm downstream from the dc discharge.

The flow conditions used in the flow tube ion source provide approximately 10^5 collisions between an ion and the buffer gas, which should thermalize the ions both rotationally and vibrationally. We assume that the internal energy of the ions produced in this source is well-described by a Maxwell−Boltzmann distribution of rotational and vibrational states corresponding to 298 K. Previous work from this laboratory has shown that this assumption is valid.[14,23−25] CID studies of $Fe(CO)^+$ and $Fe(H_2O)^+$ showed no obvious evidence of populated low-lying electronic states.

Thermochemical Analysis. Theory and experiment[26] have shown that endothermic cross sections can be modeled in the threshold region with eq 1,

$$\sigma(E) = \sigma_0 \sum g_i (E + E_{rot} + E_{vib} + E_i - E_0)^n / E \quad (1)$$

where σ_0 is an energy independent scaling factor, E is the relative translational energy of the reactants, E_{rot} is the average rotational energy of the reactants [$3kT = 0.078$ eV for $Fe(H_2O)^+ + CH_4$, C_2H_6 and $5kT/2 = 0.065$ eV for $Fe(CO)^+ + CH_4$, C_2H_6], E_{vib} is the internal energy of the neutral reactant [0.001 eV for CH_4 and 0.019 eV for C_2H_6 at 300 K as calculated using vibrational frequencies from Shimanouchi[27]], E_0 is the threshold for reaction of the ground vibrational and electronic state, and n is an adjustable parameter. The internal energy of the FeL^+ reactant ion is included explicitly as a summation over vibrational energy levels, i, with energies E_i and relative populations g_i ($\sum g_i = 1$). We assume that the relative reactivity, as reflected by σ_0 and n, is the same for all vibrational states. We use the Beyer−Swinehart[28] algorithm to calculate a Maxwell−Boltzmann distribution of vibrational energies at 298 K which is used for the factors g_i in eq 1.

The vibrational frequencies for the FeL^+ complexes used in modeling these cross sections are given in Table 1. Vibrational frequencies for $Fe(H_2O)^+$ are taken from calculations by Bauschlicher et al.[29] except for the internal modes of water, for which the frequencies for free water have been used.[27] We have estimated the sensitivity of our analysis to uncertainties in these frequencies as described in our work on $H_3O^+(H_2O)_x$ ($x = 1-5$)[24] and $M^+(H_2O)_x$ (M = Ti−Cu, $x = 1-4$).[25] All of the vibrational frequencies except for the internal modes of water were scaled by ±25%, and the corresponding change in the *average* vibrational energy is taken to be an estimate of one standard deviation of the uncertainty in vibrational energy.

At higher energies, some of the cross sections peak and then decline. To model this behavior, we use a modified form of eq 1 that accounts for a decline in the product ion cross section at higher kinetic energies. This model has been described in detail previously[30] and depends on E_D, the energy at which a dissociation channel can begin, and p, a parameter similar to n in eq 1.

Results

FeL^+ + Methane. Results for the interaction of methane with FeL^+ where L = H_2O and CO are shown in Figures 1 and 2. In both systems, we observe the four products formed in reactions 2−5.

$$FeL^+ + CH_4 \rightarrow Fe(CH_4)^+ + L + 0.73 \pm 0.06 \quad (0.77 \pm 0.08)\ \text{eV} \quad (2)$$

$$\rightarrow Fe^+ + L + CH_4 + 1.32 \pm 0.05 \quad (1.36 \pm 0.08)\ \text{eV} \quad (3)$$

$$\rightarrow LFeH^+ + CH_3 + 2.25 \pm 0.12 \quad (3.16 \pm 0.08)\ \text{eV} \quad (4)$$

$$\rightarrow FeH^+ + L + CH_3 + 3.69 \pm 0.08 \quad (3.73 \pm 0.10)\ \text{eV} \quad (5)$$

The known thermochemistry is indicated for L = H_2O (CO).[18,31]

At the lowest energies, we observe the ligand exchange product, $Fe(CH_4)^+$. In the H_2O system, this reaction is clearly

(18) Tjelta, B. L.; Armentrout, P. B. *J. Am. Chem. Soc.* **1995**, *117*, 5531.
(19) Ervin, K. M.; Armentrout, P. B. *J. Chem. Phys.* **1985**, *83*, 166.
(20) Schultz, R. H.; Armentrout, P. B. *Int. J. Mass Spec. Ion Processes* **1991**, *107*, 29.
(21) Teloy, E.; Gerlich, D. *Chem. Phys.* **1974**, *4*, 417. Gerlich, D.; Diplomarbeit, University of Freiburg, Federal Republic of Germany, 1971.
(22) Schultz, R. H.; Armentrout, P. B. *Int. J. Mass Spectrom. Ion Processes* **1991**, *107*, 29.
(23) Khan, F. A.; Clemmer, D. E.; Schultz, R. H.; Armentrout, P. B. *J. Chem. Phys.* **1993**, *97*, 7978.
(24) Dalleska, N. F.; Honma, K.; Armentrout, P. B. *J. Am. Chem. Soc.* **1993**, *115*, 12125.
(25) Dalleska, N. F.; Honma, K.; Sunderlin, L. S.; Armentrout, P. B. *J. Am. Chem. Soc.* **1994**, *116*, 3519.
(26) Aristov, N.; Armentrout, P. B. *J. Am. Chem. Soc.* **1986**, *108*, 1806 and references therein.
(27) Shimanouchi, T. *Tables of Molecular Vibrational Frequencies: Consolidated Volume I*; NSRDS-NBS 39; U.S. Government Printing Office: Washington, DC, 1972.
(28) Beyer, T.; Swinehart, D. F. *Comm. Assoc. Comput. Machines* **1973**, *16*, 379. Stein, S. E.; Rabinovitch, B. S. *J. Chem. Phys.* **1973**, *58*, 2438; *Chem. Phys. Lett.* **1977**, *49*, 183. Gilbert, R. G.; Smith, S. C. *Theory of Unimolecular and Recombination Reactions*; Blackwell Scientific: Oxford, 1990.
(29) Bauschlicher, C. W., Jr.; Langhoff, S. R.; Partridge, H.; Rice, J. D.; Komornicki, A. *J. Chem. Phys.* **1991**, *95*, 5142.
(30) Weber, M. E.; Elkind, J. L.; Armentrout, P. B. *J. Chem. Phys.* **1986**, *84*, 1521.
(31) Our previously published transition metal thermochemistry has been reevaluated in: Armentrout, P. B.; Kickel, B. L. *Organometallic Ion Chemistry*; Freiser, B. S., Ed.; Kluwer: Dordrect, 1995; pp 1−45.

Table 1. Vibrational Frequencies, cm^{-1}

species	E_{vib},[a] eV	freq, cm^{-1}
$Fe(H_2O)^+$ [b,c]	0.028(0.008)	302, 363, 438, 1694, 3824, 3913
$Fe(CO)^+$ [d]	0.030(0.011)	319, 319, 423, 2225

[a] Uncertainties are listed in parentheses, and determined as described in the text. [b] Reference 29. [c] Reference 27. [d] Ricca, A.; Bauschlicher, C. W., Jr. *J. Phys. Chem.* **1994,** *98*, 12899.

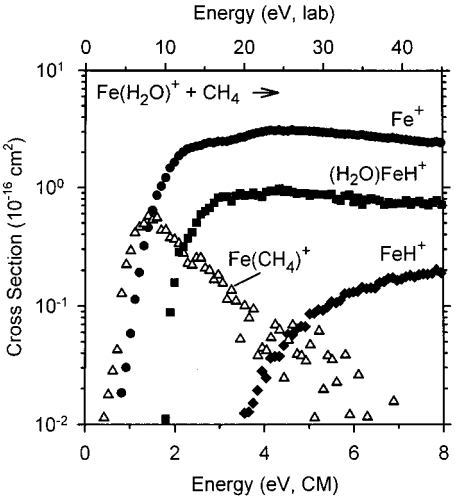

Figure 1. Cross sections for reaction of methane with $Fe(H_2O)^+$ as a function of relative kinetic energy (lower *x*-axis) and laboratory energy (upper *x*-axis).

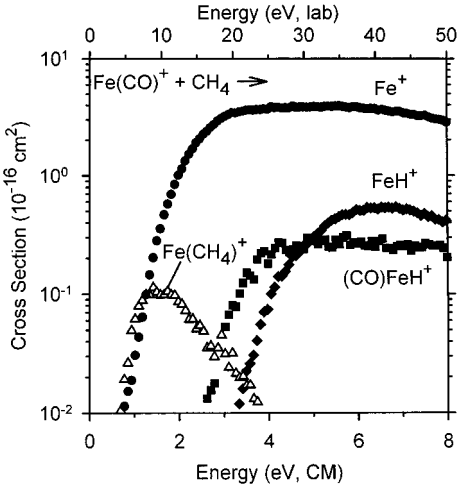

Figure 2. Cross sections for reaction of methane with $Fe(CO)^+$ as a function of relative kinetic energy (lower *x*-axis) and laboratory energy (upper *x*-axis).

endothermic with a cross section that rises to a maximum of ~0.6 Å^2. It begins to decline at the threshold for formation of Fe^+, reaction 3, an energy where the $Fe(CH_4)^+$ product can begin to decompose. In the CO system, the $Fe(CH_4)^+$ cross section exhibits a low-energy feature with a cross section of ~0.07 Å^2 at thermal energies that declines as $E^{-0.8}$, behavior consistent with an exothermic process. The magnitude of the exothermic feature depends on the ion source used, with the microwave discharge source yielding a larger exothermic feature by factors of between 2 and 4. Because the microwave source utilizes a glass discharge tube, it can be plagued by small air leaks, such that we considered whether this feature is due to an $Fe(N_2)^+$ contaminant in the beam. This can be tested by explicit examination of the $Fe(N_2)^+ + CH_4 \rightarrow Fe(CH_4)^+ + N_2$ reaction. We measure a cross section for this reaction that has the same energy dependence as the exothermic feature observed here, Figure 2, but with a cross section magnitude about 1000 times larger. Thus, the exothermic feature is consistent with a small $Fe(N_2)^+$ contaminant (~0.1%) and has been removed from the data shown in Figure 2. This contaminant is not expected to influence any of the other reaction channels observed nor is there any evidence of such problems.

At higher energies in the CO system, the $Fe(CH_4)^+$ cross section rises and reaches a peak of about 0.1 Å^2 at an energy near the onset for reaction 3. This endothermic feature is similar to the cross section for ligand exchange in the H_2O system. Using $D_0(Fe^+-CH_4) = 0.59 \pm 0.03$ eV[32] and the adiabatic BDEs of Fe^+-L,[14,15] we can calculate energy thresholds for the ligand exchange process in both systems, as indicated in reaction 2. Threshold analysis of the cross sections (after accounting for the exothermic portion in the $Fe(CO)^+$ system) yields energy thresholds of 0.82 ± 0.07 eV for $Fe(H_2O)^+$ and 0.83 ± 0.08 eV for $Fe(CO)^+$. These values are within combined experimental error of the calculated values in reaction 2. Assuming that the $Fe(CH_4)^+$ products are formed in the same electronic state in both systems (which seems likely), the consistency between the calculated and measured thresholds supports the adiabatic BDEs previously determined for the FeL^+ complexes.

The major product in both reaction systems is Fe^+, formed in the simple collision-induced dissociation (CID) reaction 3. For both systems, threshold analyses of the CID reaction with methane indicate thresholds consistent with the adiabatic BDEs, formation of $Fe^+(^6D) + L$. This is in accord with the results obtained above for the ligand exchange channels. For the CO system, the formation of Fe^+ can also occur via reaction 6,

$$Fe(CO)^+ + CH_4 \rightarrow Fe^+ + CH_3CHO + 1.62 \pm 0.08 \text{ eV} \quad (6)$$

0.26 eV higher in energy than simple CID, reaction 3. Although we cannot detect neutral species directly, a threshold analysis of the Fe^+ cross section from the CO system indicates that the lower energy process, reaction 3, is occurring. Further, although we cannot eliminate the possibility that reaction 6 contributes to the Fe^+ cross section, it seems unlikely that the complex rearrangement necessary for CH_3CHO formation will be competitive with the simple ligand dissociation, reaction 3.

As the energy is increased, the two channels involving C−H bond activation, reactions 4 and 5, are observed. The thresholds for reactions 2, 3, and 5 are similar in the two systems (consistent with the similar Fe^+-L BDEs), but the thresholds for reactions 4 differ by almost an electron volt. This leads to a much larger cross section for $(H_2O)FeH^+$ compared to $(CO)FeH^+$, Figures 1 and 2. Our analysis yields thresholds for the formation of $(H_2O)FeH^+$ of 2.25 ± 0.15 eV and for $(CO)FeH^+$ of 3.24 ± 0.24 eV. Using $D_0(H_3C-H) = 4.48 \pm 0.01$,[34] we derive LFe^+-H BDEs at 0 K of $D_0[(H_2O)Fe^+-H] = 2.23 \pm 0.15$ eV and $D_0[(CO)Fe^+-H] = 1.24 \pm 0.24$ eV. These results are consistent with and help confirm the LFe^+-D BDEs obtained in the $FeL^+ + D_2$ study,[18] Table 2. This consistency from system to system provides evidence that the reactions have neither activation barriers nor kinetic shifts.

(32) Schultz, R. H.; Armentrout, P. B. *J. Phys. Chem.* **1993**, *97*, 596.
(33) Chase, M. W., Jr.; Davies, C. A.; Downey, J. R., Jr.; Frurip, D. J.; McDonald, R. A.; Syverud, A. N. *J. Phys. Chem. Ref. Data* **1985**, *14*, Suppl. No. 1 (JANAF Tables).
(34) $\Delta_f H°_{298}(CH_4)$ and $\Delta_f H°_{298}(C_2H_6)$ taken from: Pedley, J. B.; Naylor, R. D.; Kirby, S. P. *Thermochemical Data of Organic Compounds*, 2nd ed.; Chapman and Hall: London, 1986. $\Delta_f H°_{298}(CH_3)$, $\Delta_f H°_{298}(C_2H_5)$, $\Delta_f H°_0(CH_3CO)$, and $\Delta_f H°_0(CHO)$ taken from: Berkowitz, J.; Ellison, G. B.; Gutman, D. *J. Phys. Chem.* **1994**, *98*, 2744. $\Delta_f H°_0(H)$ taken from ref 33. $\Delta_f H°_{298}$ values are converted to $\Delta_f H°_0$ by using values in: Wagman, D. D.; Evans, W. H.; Parker, V. B.; Schumm, R. H.; Halow, I.; Bailey, S. M.; Churney, K. L; Nuttall, R. L. J. *Phys. Chem. Ref. Data* **1982**, *11*, 1.

Table 2. Thermodynamic Information, eV

L =	Fe^+-L	$(H_2O)Fe^+-L$	$(CO)Fe^+-L$
D	2.15 ± 0.06^a	2.26 ± 0.12^b	1.35 ± 0.08^b
H	2.12 ± 0.06^c	2.23 ± 0.15^d	1.24 ± 0.24^d
CH_3	2.37 ± 0.05^e	1.97 ± 0.10^d	1.37 ± 0.10^d
L =	Fe^+-L	DFe^+-L	CH_3Fe^+-L
H_2O	1.32 ± 0.05^f	1.42 ± 0.14^b	0.93 ± 0.13^d
CO	1.36 ± 0.08^g	0.55 ± 0.13^b	0.36 ± 0.14^d

[a] Value derived from $D_0(Fe^+-H) = 2.12 \pm 0.06$ by adjusting for the difference in zero-point energies, 0.03 eV.[52] [b] Reference 18. [c] Reference 52. [d] This work. [e] Reference 31. [f] Reference 15. [g] Reference 14.

Table 3. Heats of Formation at 0 K

species	$\Delta_f H_0$(kJ/mol)	species	$\Delta_f H_0$(kJ/mol)
Fe^+	1173^a	CH_3CO	-3.6 ± 2.2^b
CO	113.80^a	CH_4	-66.4 ± 0.4^b
CH_3	149.8 ± 0.4^b	HCO	41.3 ± 0.8^b
C_2H_6	$-68.2_5 \pm 0.4^b$		

[a] Lias, S. G.; Bartmess, J. E.; Liebman, J. F.; Homes, J. L.; Levin, R. D.; Mallard, W. G. *J. Phys. Chem. Ref. Data, Suppl. No. 1* **1988**, *17*, 1. [b] Reference 33.

In the preceding paragraph, we assume that the structure of the $[Fe,H,C,O]^+$ product is the iron hydrido carbonyl. Another possibility is the iron formyl cation structure, $Fe(HCO)^+$. If this is the appropriate structure, then we determine an iron−formyl bond strength, $D_0(Fe^+-HCO)$, of 1.97 ± 0.25 eV from the threshold for this product and the heats of formation listed in Table 3. This is slightly smaller than the iron−methyl bond energy of $D_0(Fe^+-CH_3) = 2.37 \pm 0.05$ eV. To consider which structure is most appropriate for $[Fe,H,C,O]^+$, we note that the formation of $Fe(HCO)^+ + CH_3$ should be competitive with $FeCH_3^+ + HCO$ formation. As the $Fe(HCO)^+$ bond is weaker than the $FeCH_3^+$ bond, we would expect more of the latter products. Although not shown in Figure 2 for clarity, we do observe a very small $FeCH_3^+$ cross section with a maximum magnitude of only 0.01 Å^2 at 5 eV. Further, the $FeCH_3^+$ product can be formed in either reaction 7 or 8.

$$Fe(CO)^+ + CH_4 \rightarrow FeCH_3^+ + CO + H + 3.46 \pm 0.10 \text{ eV} \quad (7)$$

$$\rightarrow FeCH_3^+ + HCO + 2.83 \pm 0.10 \text{ eV} \quad (8)$$

A detailed analysis of the threshold for this product is complicated by the small size of its cross section and the possibility of incomplete mass resolution from the much more intense $Fe(CH_4)^+$ cross section. Nevertheless, the $FeCH_3^+$ cross section has an apparent threshold greater than 3 eV, consistent with reaction 7. Thus, all indications suggest that $[Fe,H,C,O]^+$ has the $(CO)FeH^+$ structure, although this conclusion is not definitive. In the $Fe(H_2O)^+$ system, no $FeCH_3^+$ was observed above the noise level of ~0.01 Å^2.

The results for the $HFeL^+$ products are similar to those observed in the reaction of $FeL^+ + D_2$, where $Fe(H_2O)^+$ shows enhanced reactivity for the production of $LFeD^+$. In the reaction with methane, the maximum cross section observed for the production of $(H_2O)FeH^+$ is about 0.9 Å^2 compared to a cross section maximum for $(CO)FeH^+$ of about 0.3 Å^2. The cross section magnitudes are about twice as large as those observed in the D_2 reaction.[18] In the D_2 reaction,[18] it is clear that the $LFeD^+$ and FeD^+ channels are coupled because the cross section for the $LFeD^+$ product begins to decline at about 3.5 eV, the threshold for formation of FeD^+. In the methane system, however, the cross sections for the $LFeH^+$ product remain roughly constant above 4 eV. Given that $D_0(D-D)$[33] ≈ $D_0(H_3C-H)$,[34] the observed behavior implies that the methyl radical product in reaction 4 carries away much more of the excess available energy, either in internal modes or in translation, something which the D atom product cannot do easily.

For the FeH^+ product channel, we observe similar thresholds in the $Fe(H_2O)^+$ and $Fe(CO)^+$ systems (consistent with similar Fe^+-L BDEs). In the CO system, FeH^+ might also be accompanied by the acetyl neutral product formed in reaction 9.

$$Fe(CO)^+ + CH_4 \rightarrow FeH^+ + CH_3CO + 3.32 \pm 0.10 \text{ eV} \quad (9)$$

This pathway is 0.41 ± 0.14 eV lower in energy than reaction 5. A threshold analysis of the FeH^+ cross section for L = CO yields 4.07 ± 0.15 eV, a value slightly higher than the thermodynamic threshold calculated for reaction 5, 3.73 ± 0.10 eV. Alternatively, we note that we can reproduce the cross section with eq 1 with E_0 held to 3.73 eV, but not 3.32 eV. Neither do we observe any evidence of a low-energy feature in the FeH^+ cross section that would indicate the formation of the CH_3CO neutral.

The cross section magnitude for FeH^+ is about 3 times larger in the $Fe(CO)^+$ system. This is primarily an indication of the relative stabilities of $LFeH^+$. $(CO)FeH^+$, having fewer vibrational modes than $(H_2O)FeH^+$, decomposes more readily at higher energies. In contrast, the cross section for the sum of the FeH^+ and $LFeH^+$ cross sections is ~1 Å^2 above 6 eV for both FeL^+ reactants in the methane system. The cross section sum can be viewed as the cross section for *formation* of $LFeH^+$ and is probably a better reflection of the overall probability of C-H bond activation because the stability of the $LFeH^+$ products is no longer an issue.

Similar to the $LFeH^+$ product, we also expected that we might observe the $LFeCH_3^+$ product. Despite a careful search, this product was not observed and is assumed to be below our noise level in these experiments. This is reasonable given that the reaction of atomic Fe^+ with methane produces less $FeCH_3^+$ than FeH^+ by a factor of about 40.[11]

FeL^+ + Ethane. As in the reactions with methane, the reactions of FeL^+ with ethane yield four major product channels, reactions 10−13.

$$FeL^+ + C_2H_6 \rightarrow Fe(C_2H_6)^+ + L + 0.66 \pm 0.08 \quad (0.70 \pm 0.10) \text{ eV} \quad (10)$$

$$\rightarrow Fe^+ + L + C_2H_6 + 1.32 \pm 0.05 \quad (1.36 \pm 0.08) \text{ eV} \quad (11)$$

$$\rightarrow LFeH^+ + C_2H_5 + 2.08_5 \pm 0.12 \quad (3.00 \pm 0.08) \text{ eV} \quad (12)$$

$$\rightarrow FeH^+ + L + C_2H_5 + 3.52 \pm 0.08 \quad (3.58 \pm 0.10) \text{ eV} \quad (13)$$

The results are shown in Figures 3a and 4a. At the lowest energies, we observe the ligand exchange product, $Fe(C_2H_6)^+$. In the H_2O system, the reaction is clearly endothermic with a cross section that rises to a maximum of ~2 Å^2. It begins to decline at the threshold for formation of Fe^+, reaction 11, an energy where the $Fe(C_2H_6)^+$ product decomposes. In the CO system, the $Fe(C_2H_6)^+$ cross section exhibits a low-energy feature with a cross section of ~0.14 Å^2 at thermal energies

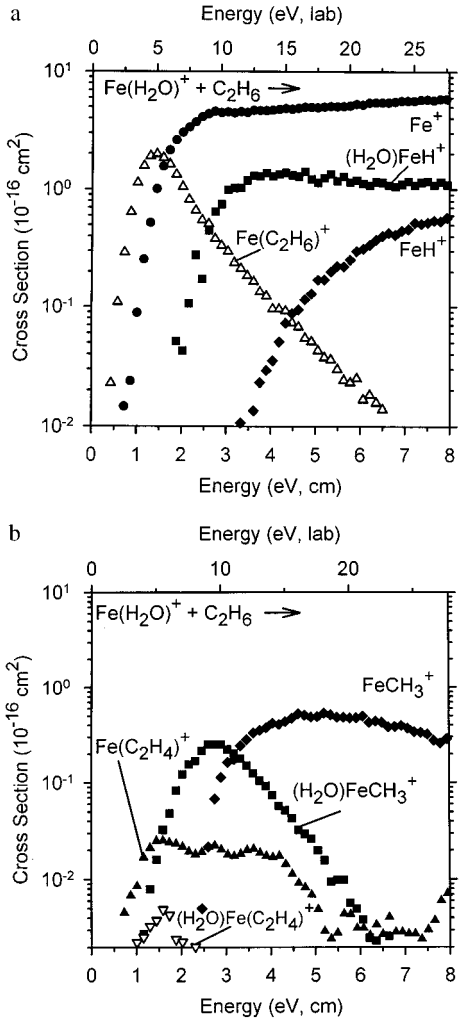

Figure 3. Cross sections for reaction of $Fe(H_2O)^+$ and ethane as a function of kinetic energy in the center-of-mass frame (lower scale) and laboratory frame (upper scale). Note the different cross section scales in parts a and b.

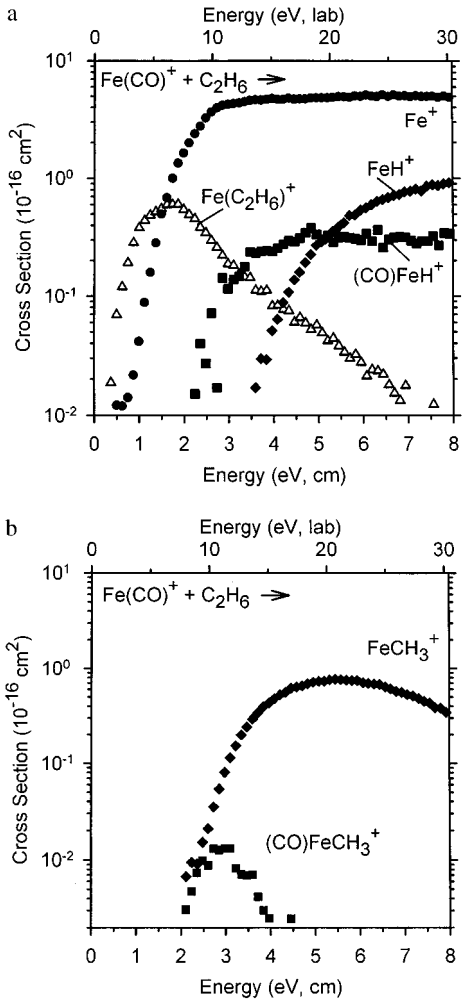

Figure 4. Cross sections for reaction of $Fe(CO)^+$ and ethane as a function of kinetic energy in the center-of-mass frame (lower scale) and laboratory frame (upper scale). Note the different cross section scales in parts a and b.

that behaves like an exothermic process. As in the methane system, this exothermic feature is believed to be the result of a small amount of $Fe(N_2)^+$ present in the beam and has therefore been removed from the data shown. At higher energies, the $Fe(C_2H_6)^+$ cross section exhibits a cross section peak of about 0.6 Å^2 that occurs near the onset of reaction 11, again due to competition.

The major product in both cases is Fe^+, formed in the simple CID reaction 11. As in the methane system, threshold analysis of these Fe^+ cross sections indicates thresholds consistent with the adiabatic bond dissociation energies for both ligands. In the CO system, it is also possible that Fe^+ is accompanied by formation of neutral acetone, reaction 14.

$$Fe(CO)^+ + C_2H_6 \rightarrow Fe^+ + (CH_3)_2CO + 1.17 \pm 0.08 \text{ eV} \quad (14)$$

This process is 0.19 ± 0.11 eV lower in energy than the CID process, reaction 11. Our threshold analysis of the Fe^+ cross section from $Fe(CO)^+$ yields an energy threshold of 1.27 ± 0.09 eV, within experimental error of the calculated thresholds of both reactions 11 and 14. Although we cannot rule out the possibility of reaction 14 based on the threshold, a comparision of the Fe^+ product channels for the methane and ethane systems indicates cross sections with small differences in absolute magnitude but identical kinetic energy dependence for over two orders of magnitude throughout the threshold region. Additionally, comparison of the Fe^+ product channels with ethane for the CO and H_2O systems indicates no evidence for a low-energy feature in the CO system that would indicate that formation of acetone in reaction 14 is occurring. As the experimental observations are perfectly consistent with simple CID, reaction 11, it seems unlikely that the more complex rearrangement in reaction 14 would make a significant contribution to the observed cross section, although a minor contribution cannot be ruled out either.

The Fe^+ cross sections rise to a maximum cross section of about 5.5 Å^2, about 1.5 times larger than in the methane system. As the energy is increased, the two channels involving C−H activation, reactions 12 and 13, are observed. It can be seen that the thresholds for reactions 10, 11, and 13 are similar in the two systems (consistent with the similar Fe^+−L BDEs), but the thresholds for reaction 12 differ by almost an electron volt. This leads to a much larger cross section for $(H_2O)FeH^+$ compared to $(CO)FeH^+$. Both the thresholds and cross section magnitudes of these products are similar to the methane results. The cross section for the $LFeH^+$ product is more difficult to model in the ethane than in the dihydrogen and methane systems. As a result, an independent measure of the $LFe-H^+$ BDE is not obtained from these data, although the cross sections for reactions 12 can be reproduced using eq 1 and thresholds calculated from the LFe^+-H BDEs measured in the D_2 and CH_4 systems.

In the CO system, we might also consider whether the (CO)FeH^+ product is really $FeC_2H_5^+$, which has the same nominal mass, or has the structure $Fe(HCO)^+$. The latter possibility is discounted for the same reasons outlined in the methane reaction. The iron ethyl cation can be formed in either reaction 15 or 16. The former process has a threshold inconsistent with that measured for this product ion, while the latter is within experimental error of the measured threshold.

$$Fe(CO)^+ + C_2H_6 \rightarrow FeC_2H_5^+ + CO + H + 3.26 \pm 0.13 \text{ eV} \quad (15)$$

$$\rightarrow FeC_2H_5^+ + HCO + 2.73 \pm 0.13 \text{ eV} \quad (16)$$

In this case, we discount appreciable contributions of reaction 16 to the observed cross section because the comparable process was not observed in the methane system. Overall, we cannot eliminate the possibilties that $Fe(HCO)^+$ and $FeC_2H_5^+$ contribute to the (CO)FeH^+ cross section, but the observed behavior is most easily interpreted solely with production of (CO)FeH^+.

For the FeH^+ product channel, the cross section magnitude is about 3 times larger in the $Fe(CO)^+$ system than in the $Fe(H_2O)^+$ system. As discussed above, this behavior can be understood in terms of the stability of the $LFeH^+$ precursor. The cross section for the formation of $LFeH^+$ (the sum of the $LFeH^+$ and FeH^+ cross sections) is ~1.2 Å^2 above 6 eV for both ligands, comparable magnitudes to the methane system. In the CO system, the neutral products accompanying FeH^+ could also be the C_2H_5CO radical formed in reaction 17.

$$Fe(CO)^+ + C_2H_6 \rightarrow FeH^+ + C_2H_5CO + 3.07 \pm 0.11 \text{ eV} \quad (17)$$

If we estimate $\Delta_f H°(C_2H_5CO)$ on the basis of its methyl analogue, acetyl radical, we calculate that reaction 17 is a lower energy pathway than reaction 13 by >0.5 eV. As in the methane system, we do not see evidence of a low-energy feature that would positively identify this process.

In addition to reactions 10−13, we observe two additional reaction channels involving C−C bond activation, reactions 18 and 19, in both systems (Figures 3b and 4b).

$$FeL^+ + C_2H_6 \rightarrow FeCH_3^+ + L + CH_3 + 2.76 \pm 0.07 \ (2.80 \pm 0.09) \text{ eV} \quad (18)$$

$$\rightarrow LFeCH_3^+ + CH_3 \quad (19)$$

The thresholds observed for reactions 18 are similar in the two systems, but the thresholds for reactions 19 are quite different, consistent with the behavior in the analogous C−H bond activation channels. For the CO system, the $FeCH_3^+$ product might also be accompanied by the acetyl radical, reaction 20.

$$Fe(CO)^+ + C_2H_6 \rightarrow FeCH_3^+ + CH_3CO + 2.39 \pm 0.09 \text{ eV} \quad (20)$$

This has a threshold 0.41 ± 0.13 eV lower in energy than reaction 18. We measure similar thresholds for $FeCH_3^+$ in both the H_2O and CO systems, 2.88 ± 0.19 and 2.78 ± 0.17 eV, respectively. These values are consistent with the thermodynamic thresholds of reactions 18, such that there is no indication that process 20 occurs. (Although the logarithmic display of these data in Figure 4b makes it appear that the $FeCH_3^+$ cross section has a threshold comparable to (CO)$FeCH_3^+$, this is because the $FeCH_3^+$ cross section is larger by about two order of magnitude such that kinetic energy broadening decreases the apparent threshold well below that determined from analysis. Equation 1 with $E_0 = 2.78$ eV reproduces the $FeCH_3^+$ cross section throughout the threshold region within experimental uncertainties.)

The $(H_2O)FeCH_3^+$ product channel has a much larger cross section (maximum of 0.25 Å^2) compared to (CO)$FeCH_3^+$ (maximum of 0.012 Å^2). However, as in the C−H bond activation channels, the magnitudes of the sum of the $FeCH_3^+$ and $LFeCH_3^+$ cross sections for both systems are comparable, ~0.6 Å^2 at higher energies. It is clear that the $LFeCH_3^+$ and $FeCH_3^+$ channels are coupled because the cross sections for the $LFeCH_3^+$ products begin to decline at about 2.8 eV, the threshold for ligand loss to form $FeCH_3^+$.

Analyses of reaction 19 with eq 1 yield thresholds for the formation of $(H_2O)FeCH_3^+$ of 1.84 ± 0.10 eV and for (CO)$FeCH_3^+$ of 2.44 ± 0.10 eV. Assuming no barrier to reaction in excess of the endothermicity, these thresholds can be converted to the LFe^+-CH_3 BDEs given in Table 2 using $D_0(H_3C-CH_3) = 3.806 \pm 0.007$ eV.[34] Alternatively, it is possible that the (CO)$FeCH_3^+$ ion has an iron acetyl cation structure, $Fe(CH_3CO)^+$, instead. Using the threshold obtained in reaction 19 and the heats of formation listed in Table 3, this assumption leads to a bond energy of $D_0(Fe^+-COCH_3) = 2.32 \pm 0.13$ eV, which is similar to $D_0(Fe^+-CH_3) = 2.37 \pm 0.05$ eV. Noting that formation of $FeCH_3^+ + CH_3CO$ should compete directly with $Fe(CH_3CO)^+ + CH_3$, the relative thermochemistry suggests that comparable amounts of these two products would be seen, in contrast to our observations. Further, our failure to observe reaction 20 discounts any appreciable production of an acetyl moeity. Thus, all indications are that reaction 19 forms (CO)$FeCH_3^+$, where the ligand is largely a spectator in the reaction. This conclusion is supported by the observation that the $LFeCH_3^+$ and $FeCH_3^+$ channels are strongly coupled in both the CO and H_2O systems. This indicates that loss of the ligand L from the primary $LFeCH_3^+$ product gives rise to the $FeCH_3^+$ cross section.

Dehydrogenation processes, reactions 21 and 22, are observed in the $Fe(H_2O)^+$ system (Figure 3b).

$$Fe(H_2O)^+ + C_2H_6 \rightarrow Fe(C_2H_4)^+ + H_2O + H_2 + 1.16 \pm 0.08 \text{ eV} \quad (21)$$

$$\rightarrow (H_2O)Fe(C_2H_4)^+ + H_2 \quad (22)$$

In the $Fe(CO)^+$ system, we are unable to monitor the analogue of reaction 21 because the dehydrogenation product, $Fe(C_2H_4)^+$, has the same mass-to-charge ratio as the reactant ion beam. No (CO)$Fe(C_2H_4)^+$ was observed despite a careful search.

A low-energy feature consistent with an exothermic process and with a cross section of ~0.5 Å^2 at thermal energies was observed in the $Fe(C_2H_4)^+$ cross section. Comparison of these data to that for the reaction $Fe(H_2O)^+ + C_2H_4 \rightarrow Fe(C_2H_4)^+ + H_2O$ examined previously in our laboratory[35] shows that the exothermic feature in our $Fe(C_2H_4)^+$ cross section is due to ethene contamination in the ethane. Thus, we have removed the cross section associated with the ethene contamination, yielding the cross section shown in Figure 3b. The remaining cross section has an apparent threshold less than 1 eV, rises to a maximum cross section magnitude of ~0.025 Å^2 at about 1.5 eV, and does not decline until almost 4.5 eV. This broad peak shape is attributed to competition with other reactions, as discussed further below. A threshold analysis of the $Fe(C_2H_4)^+$ cross section yields E_0 values between 0.9 and 1.4 eV, a range

(35) Dalleska, N. F. Thesis, University of Utah, 1993.

that encompasses the calculated value indicated in reaction 21. The ligated dehydrogenation product, $(H_2O)Fe(C_2H_4)^+$, exhibits a very small cross section, less than ~0.01 Å^2, with an energy threshold measured to be 0.67 ± 0.12 eV. The small size of the product cross section can be attributed to decomposition of this product in the overall reaction 21.

Discussion

Failure To Observe Coupling of Alkane with CO Ligand. In the previous section, we found no evidence that the CO ligand participates directly in the C−H and C−C bond activation reactions and could exclude such participation in several processes. The failure to observe coupling with the CO ligand obtains even though formation of $COCH_3$, COC_2H_5, and $CO(CH_3)_2$ as neutral products are lower energy processes than production of CH_3 + CO, C_2H_5 + CO, and C_2H_6 + CO, respectively. We can begin to understand this on the basis of recent experimental studies of the reactions of Fe^+, Co^+, and Ni^+ with acetone. It has long be known that these metal ions react with acetone to form both MCO^+ and $MC_2H_6^+$.[36,37] The recent study confirms that the $MC_2H_6^+$ species is the metal−ethane cation rather than a dimethyl complex and further characterizes the potential energy surface for these reactions.[38] On this surface, the lowest energy species is the $CO-M^+-C_2H_6$ adduct. For M = Co, this adduct is estimated to lie 1.65 eV lower in energy than the C−C insertion transition state, $CH_3-M^+-COCH_3$. This estimate is based on comparisons with thermochemistry of a bare Co^+ metal center inserting into ethane or propane, and does not explicitly consider how the CO ligand might affect this thermochemistry. As discussed below, the presence of the CO ligand impedes activation of σ-bonds, which suggests that the $CH_3-Co^+-COCH_3$ insertion species may lie even higher in energy. Further, to form M^+(acetone) requires passing over at least two tight transition states corresponding to CO insertion into the C−C bond of ethane and methyl transfer from the metal to the carbonyl.

When this surface is entered from the M^+ + acetone side, it is exothermic to eliminate CO or ethane and these are the only low-energy processes available. Thus, the rearrangement of acetone to CO + C_2H_6 induced by M^+ is facile. When the reaction starts at MCO^+ + C_2H_6, it is now endothermic to reach the tight transition states leading to acetone formation and there is strong competition with the kinetically favored ligand exchange and CID processes. Thus, the rearrangement of CO + C_2H_6 to acetone induced by M^+ is sufficiently inefficient that it is not observed. At higher energies, the cleavage of the C−C bond to form $(CO)MCH_3^+$ can occur by more direct pathways that need not involve intermediates such as $(CO)M^+(CH_3)_2$ or $(CH_3)M^+(COCH_3)$. One would anticipate that coupling of the carbonyl ligand to the hydrocarbon reactant would become more efficient as the endothermicity of such coupling reactions decreases and as the lifetime of the intermediates increases. Both effects occur as the complexity of the alkane reactant increases, as verified by studies of the reaction of $FeCO^+$ with propane.[39] We observe a detectable amount of CO coupling (~5% of the CID cross section) at low energies in the propane system. This study verifies that we can experimentally observe the results of coupling reactions when they are significant; however, we are probably insensitive to such reactions at a level below 1% of the CID cross section.

Reaction Efficiency. As for CID with D_2 and He,[18] collisions with methane and ethane induce adiabatic dissociation of $Fe(CO)^+(^4\Sigma^-)$ to $Fe^+(^6D)$ + $CO(^1\Sigma^+)$. These spin-forbidden dissociations differ from the behavior observed when Xe is used as the collision gas, where spin-allowed dissociation to form $Fe^+(^4F)$ + CO is observed.[14] Although further studies of these different behaviors are needed to elucidate this behavior, two effects could be involved. First, the more complex molecular collision partners involve potential energy surfaces and surface interactions of higher dimensionality, which probably enhances adiabatic behavior. Second, the mechanism for the simpler atomic cases may then be determined by the details of the quartet−sextet surface interactions. $FeXe^+$ has been calculated to have a quartet ground state[40] while $FeHe^+$ is found to be a sextet.[41] Thus, collisions of $Fe(CO)^+(^4\Sigma^+)$ with Xe may preferentially remain on a quartet surface while those with He may allow greater mixing between the two spin states.

The maximum cross section magnitudes for CID of FeL^+ with dihydrogen and helium are about half those obtained with methane and ethane, which are comparable to those with Xe. Changes in estimated hard-sphere and ion-induced dipole collision cross sections account for some of this difference, although the trend is not quantitatively predicted. An additional effect is longer-lived intermediates for the species with higher polarizabilities, i.e. the alkanes and Xe. This should make the energy transfer in the collision more efficient and thus enhance the CID probability.[42,43]

As noted above, $Fe(H_2O)^+$ exhibits enhanced reactivity compared to $Fe(CO)^+$ in the ligand exchange product channels in the methane and ethane systems, reactions 2 and 10. Fe^+−alkane complexes have been calculated to have quartet ground states.[44] Therefore, we might have expected to observe a larger cross section for the spin-allowed process, $Fe(CO)^+(^4\Sigma^-)$ + $C_nH_{2n+2}(^1A)$ → $Fe(C_nH_{2n+2})^+(^4E)$ + $CO(^1\Sigma^+)$. Instead, we observe a larger cross section magnitude for the spin-forbidden process, $Fe(H_2O)^+(^6A_1)$ + $C_nH_{2n+2}(^1A)$ → $Fe(C_nH_{2n+2})^+(^4E)$ + $H_2O(^1A_1)$. We can begin to understand this observation by considering the intermediate complex, $LFe(C_nH_{2n+2})^+$, almost certainly a quartet in both systems.[45] There are two dissociation pathways for this intermediate, formation of $Fe(C_nH_{2n+2})^+$ + L and formation of FeL^+ + C_nH_{2n+2}, where the latter is the thermodynamically favored pathway for both ligands. For L = H_2O, it seems likely that the intermediate will preferentially dissociate by the spin-allowed process to form $Fe(C_nH_{2n+2})^+$ when energetically feasible. For L = CO, both pathways are spin-allowed such that competition between the two channels is more severe, thus, the cross section for $Fe(C_nH_{2n+2})^+$ is less probable in the CO system than for L = H_2O.

Thermochemistry. Results obtained here and in the reactions with D_2[18] indicate that the CO ligand greatly diminishes the Fe^+-R (R = H, D, or CH_3) BDEs compared to the unligated metal ion, while the H_2O ligand has a much smaller effect on these BDEs (Table 2). Concomitantly, covalently bonding an R group to Fe^+ destabilizes the metal−CO interaction while leaving the metal−water binding largely intact. This difference can be understood by examining the electronic configuration of the metal−ligand complexes. The ground state of $Fe(H_2O)^+$

(36) Halle, L. F.; Crowe, W. E.; Armentrout, P. B.; Beauchamp, J. L. *Organometallics* **1984**, *3*, 1694.
(37) Burnier, R. C.; Byrd, G. D.; Freiser, B. S. *J. Am. Chem. Soc.* **1981**, *103*, 4360.
(38) Carpenter, C. J.; van Koppen, P. A. M.; Bowers, M. T. *J. Am. Chem. Soc.* **1995**, *117*, 10976.
(39) Tjelta, B. L.; Armentrout, P. B. *J. Am. Chem. Soc.* Submitted for publication.
(40) Heinemann, C.; Schwarz, J.; Koch, W.; Schwarz, H. *J. Chem. Phys.* **1995**, *103*, 4551.
(41) Partridge, H.; Bauschlicher, C. W., Jr.; Langhoff, S. R. *J. Phys. Chem.* **1992**, *96*, 5350. Partridge, H.; Bauschlicher, C. W., Jr. *J. Phys. Chem.* **1994**, *98*, 2301.
(42) Aristov, N.; Armentrout, P. B. *J. Phys. Chem.* **1986**, *90*, 5135.
(43) Hales, D. A.; Armentrout, P. B. *J. Cluster Sci.* **1990**, 127.
(44) Perry, J. K. Thesis, California Institute of Technology, 1993.
(45) This seems probable given that $Fe^+(H_2O)_2$ is calculated to have a $^4B_{1g}$ ground state.[17]

is $^6A_1$ with an Fe^+ occupation of $4s^13d\sigma^13d\pi^23d\delta^3$ derived from the $^6D(4s^13d^6)$ ground state of Fe^+.[17] The repulsion between the occupied 4s orbital and the electron donating water ligand is reduced by mixing in 4p character such that the 4s orbital is polarized away from the ligand.[17] In contrast, the ground state of $Fe(CO)^+$ is $^4\Sigma^-$ with an Fe^+ occupation of $3d\sigma^13d\pi^43d\delta^2$ derived from the $^4F(3d^7)$ state of Fe^+.[16] The bonding here involves 4s to 3d promotion as well as some 4s−3dσ hybridization in order to reduce the repulsion between the metal 3d and 4s electrons and the CO 5σ electrons.[16]

It is known that the first-row transition metal ions use the 4s orbital to bind hydrogen atoms and methyl radicals.[46,47−52] $Fe(H_2O)^+$ can use the electron in the 4s−4p orbital that is polarized away from the incoming ligand to form a strong covalent bond with the R groups. This should give a pseudo-linear $(H_2O)FeR^+$ structure. In contrast, $Fe(CO)^+$ does not have a 4s electron. Formation of $(CO)FeR^+$ presumably involves binding R to the 3dσ molecular orbital (resulting in a weaker bond than for a covalent interaction with the 4s orbital and a ~90° $(CO)FeR^+$ structure) or $Fe(CO)^+$ must promote an electron to a 4s orbital which costs energy and weakens the Fe^+−CO interaction. Indeed, the RFe^+−CO BDEs are comparable to the binding energy for CO to the ^6D state of Fe^+.[16]

The bond strength of $(H_2O)Fe^+-CH_3$ is 0.29 eV smaller than that of $(H_2O)Fe^+$−D, whereas $D_0[(CO)Fe^+-CH_3] \approx D_0[(CO)Fe^+-D]$ (Table 2), and $D_0(Fe^+-CH_3)$ is 0.21 eV larger than $D_0(Fe^+-D)$. We can understand this by noting that a methyl group is a more polarizable ligand than a deuterium atom and is also a weak π-donor. These effects explain the relative binding energies to the atomic ions. For $Fe(H_2O)^+$, the H_2O ligand destabilizes the Fe^+-CH_3 interaction because both ligands are π-donors. On the other hand, CO is a π-acceptor which could allow a synergistic binding effect with CH_3. We believe that $Fe(CO)^+$ cannot take advantage of the π-donating ability of CH_3 because the 3dπ orbitals in this case are already filled.[16]

The dehydrogenation of ethane to form $(H_2O)Fe(C_2H_4)^+$ exhibits an endothermic cross section yielding an energy threshold of 0.67 ± 0.12 eV. If we assume that $D_0[(C_2H_4)Fe^+-(H_2O)] \approx D_0[(H_2O)Fe^+-(H_2O)] = 1.70 \pm 0.04$ eV,[15] then formation of $(H_2O)Fe(C_2H_4)^+$ in reaction 22 should be exothermic by ~0.5 eV. This assumption is reasonable because both C_2H_4 and H_2O are σ-donating ligands although some differences are expected because of the different π character of the ligands. Nevertheless, it seems certain that the $(H_2O)Fe(C_2H_4)^+$ energy threshold is a measure of a barrier height rather than the endothermicity associated with its formation. This seems reasonable as dehydrogenation of C_2H_6 by atomic Fe^+ also shows a barrier.[48,49,50] At higher energies, the $(H_2O)Fe(C_2H_4)^+$ product goes on to lose the H_2O ligand to form $Fe(C_2H_4)^+$. The threshold for this process is consistent with the calculated thermodynamic value given in eq 21, which indicates that there is no barrier to formation of the $Fe(C_2H_4)^+$ product. This is expected as long as the thermodynamic threshold for reaction 21 is greater than the barrier height, i.e., the threshold of reaction 22 is less than that for reaction 21, as measured here.

Effects of Ligation on C−H and C−C Bond Activation Reactivity. In addition to the thermochemistry discussed above, we can also deduce information about the mechanisms of reaction. The general results observed in the methane and ethane systems are similar to those we observed for reaction of D_2 with FeL^+.[18] In that case, the results were rationalized using molecular orbital (MO) arguments similar to those developed to explain the state-specific reactivity of atomic iron ions.[11,51] A general approach can be used because the reactions of interest are all σ-bond activations: either of D_2, the C−H bond of methane or ethane, or the C−C bond of ethane. Further, the BDEs of these bonds are fairly similar: $D_0(D_2) = 4.556 \pm 0.001$ eV,[33] $D_0(H-CH_3) = 4.477 \pm 0.005$ eV,[34] $D_0(H-C_2H_5) = 4.31_5 \pm 0.02$ eV,[34] and $D_0(H_3C-CH_3) = 3.806 \pm 0.007$ eV.[34]

The relative reactivities of $Fe(CO)^+$ and $Fe(H_2O)^+$ observed here are somewhat surprising if one imagines that the $Fe(CO)^+(^4\Sigma^-)$ should react similarly to the more reactive $Fe^+(^4F)$ and that $Fe(H_2O)^+(^6A_1)$ should react similarly to the less reactive $Fe^+(^6D)$. Although the cross sections for $(H_2O)FeR^+$ (R = H or CH_3) are larger than those for $(CO)FeR^+$, this is largely because the latter species decomposes more readily, as discussed above. A better measure of the bond activation probability is the *sum* of the $LFeR^+$ and FeR^+ cross sections. In this case, the cross sections for the formation of $LFeR^+$ are of similar magnitude in both the H_2O and CO systems. Further, they are between those observed for production of FeR^+ in the reaction of the two electronic states of atomic Fe^+ with CH_4 and C_2H_6.[11]

As discussed elsewhere,[4,52] σ-bond activation at a metal center can be thought of as a process in which the σ-bonding orbital donates electron density into an acceptor orbital on the metal and the metal back donates π-electron density into the antibonding σ^* orbital. For first-row atomic transition metal ions, the acceptor orbital is largely 4s and the donor is 3dπ. Thus, $Fe^+(^4F,3d^7)$ is more reactive than $Fe^+(^6D,4s^13d^6)$ because the acceptor orbital is empty in the former state and occupied in the latter. The characteristics of the acceptor orbitals in the ligated species are harder to ascertain because CO and H_2O are both σ-donating ligands. It seems likely that the acceptor orbital in $Fe(CO)^+$ is the singly occupied 4s−3dσ hybrid MO because the other 4s−3dσ hybrid MO is already accepting two electrons from the CO ligand (and it is unfavorable to donate the σ-bonding electrons into the antibonding Fe−CO orbital). In $Fe(H_2O)^+$, the likely acceptor is the singly occupied 4s−4p MO polarized away from the ligand. The FeL^+ complexes are less reactive than $Fe^+(^4F)$ because the acceptor orbitals are singly occupied in the ligated species rather than empty. The σ-accepting ability of these MOs on FeL^+ vs the 4s orbital on $Fe^+(^6D)$ must explain in part the reactivity enhancement of the FeL^+ species compared to $Fe^+(^6D)$. For the ligated Fe^+ ions, the π-back donation necessary to activate the σ-bond should be enhanced by the π-donating H_2O ligand and suppressed by the π-accepting CO ligand. Because the reactivities of the FeL^+ species are comparable at higher energies, this would suggest that the σ-accepting abilities of FeL^+ provide the primary determination of the reactivity (which is reasonable because the

(46) Schilling, J. B.; Goddard, W. A.; Beauchamp, J. L. *J. Am. Chem. Soc.* **1986**, *108*, 582.

(47) Pettersson, L. G. M.; Bauschlicher, C. W.; Langhoff, S. R.; Partridge, H. *J. Chem. Phys.* **1987**, *87*, 481.

(48) In contrast to previous reports from our laboratory,[11] new studies indicate that the $Fe^+(^6D)$ ground state does *not* dehydrogenate ethane exothermically, although this process is observed at higher kinetic energies with a very small cross section (maximum of 0.002 Å^2 at 2−3 eV). It seems likely that our previous observation was of the reaction of a high-lying excited state of Fe^+ generated by electron impact that was not quenched in the drift cell source used.[49,50] Our previous work shows that $Fe^+(^4F)$ reacts with ethane to eliminate H_2 once an energy threshold of 0.2−0.5 eV is overcome.[11] In analogy to more detailed studies on the $Co^+ + C_2H_6$ system,[51] this threshold is attributed to a barrier along the potential energy surface.

(49) Oreido, J. V. B.; Russel, H. *J. Phys. Chem.* **1992**, *96*, 5314.

(50) Loh, S. K.; Fisher, E. R.; Lian, L.; Schultz, R. H.; Armentrout, P. B. *J. Phys. Chem.* **1989**, *93*, 3159.

(51) Haynes, C. L.; Fisher, E. R.; Armentrout, P. B. *J. Am. Chem. Soc.* **1996**, *118*, 3269.

(52) Elkind, J. L.; Armentrout, P. B. *J. Am. Chem. Soc.* **1986**, *108*, 2765. Elkind, J. L.; Armentrout, P. B. *J. Phys. Chem.* **1986**, *90*, 5736.

Scheme 1

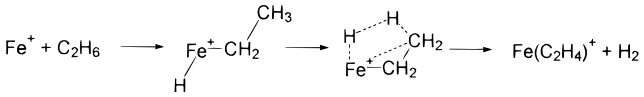

σ interaction should be longer range than the π interaction) or that a balance between the σ-accepting and π-donating abilities is attained in the complexes.

Effects of Ligation on the Dehydrogenation of Ethane. The most dramatic ligand effects are observed in the dehydrogenation of ethane to form $LFe(C_2H_4)^+$, a process that involves activation of two σ-bonds. Dehydrogenation of ethane is not observed for the reactions of ground state $Fe^+(^6D)$[48] and $Fe(CO)^+(^4\Sigma^-)$, and small cross sections are observed for the dehydrogenation by excited state $Fe^+(^4F)$ and $Fe(H_2O)^+(^6A_1)$. The cross section for formation of $(H_2O)Fe(C_2H_4)^+$ has a cross section magnitude <0.01 Å^2, about half that for the reaction of $Fe^+(^4F)$. Further, the ligated species exhibits a slightly larger barrier to reaction, 0.67 ± 0.12 eV, compared to the atomic ion, 0.2−0.5 eV.[11,48]

On the basis of recent experimental studies of the analogous Co^+ reactions[51] and theoretical studies of both the Co^+ and Fe^+ reactions,[44,53] it is now believed that the mechanism for dehydrogenation first involves insertion of Fe^+ into a C−H bond to form $H-Fe^+-C_2H_5$ (Scheme 1). Then a five-center transition state activates the second C−H bond while simultaneously forming H_2. This leads to a $(H_2)Fe(C_2H_4)^+$ intermediate (an η^2 H_2 complex, not a dihydride) that easily loses H_2. The calculations identify the multicentered transition state as rate determining. To understand the differences in reactivity observed upon ligation, we can consider how ligation affects the stability of the $H-Fe^+-C_2H_5$ and $(H_2)Fe(C_2H_4)^+$ intermediates and the multicenter transition state.

Perry[44] has recently discussed a similar problem in comparing the reactivity of H_2 with the bare Co^+ ion and $Co(C_2H_4)^+$.[51] He notes that in order to efficiently activate H_2 and form two strong Co−H bonds, the Co^+ center must utilize 4s−3d hybridization such that each hybrid can be used to form a bond between Co and a hydrogen atom. When this occurs with $Co(C_2H_4)^+$, however, the 4s orbital has a repulsive interaction with the ethene ligand. In the present system, we also presume that 4s−3d hybridization is necessary to activate the C−H bond of ethane and form the $HFeC_2H_5^+$ intermediate. The CO ligand disrupts this process considerably because it also requires 4s−3d hybridization to form a strong Fe^+-CO bond. Because the H_2O ligand utilizes 4p character instead, this disruption can be minimized.

For the $(H_2)Fe(C_2H_4)^+$ intermediate, we simply note that the third ligand in both the $Fe(CO)_x^+$ and $Fe(H_2O)_x^+$ series is more weakly bound than the first two ligands.[14,15] This is because the hybridizations that are used to enhance the metal−ligand bonds can no longer be used effectively for the third ligand. Hence, ligation is expected to destabilize the $(H_2)Fe(C_2H_4)^+$ intermediate. Presumably, ligation should also adversely affect the stability of the five-center transition state, although this is more difficult to analyze in detail. Certainly, we find that the barrier associated with the five-center transition state increases by 0.3 ± 0.2 eV upon ligation with H_2O, and could be much higher upon ligation with CO. The difference in the barrier heights provides direct evidence that ligation does destabilize this transition state.

Product Branching Ratios. In the case of methane, evidence in support of a direct mechanism for the reaction of FeL^+ and CH_4 comes from the $FeH^+/FeCH_3^+$ branching ratios of $\sim$ 43:1 observed for $Fe(CO)^+ + CH_4$. The branching ratio for $[FeH^+ + (CO)FeH^+]/[FeCH_3^+ + (CO)FeCH_3^+]$ is about 70:1. This large branching ratio occurs even though the thermodynamic threshold for production of $FeCH_3^+$ is 0.33 eV lower than that for FeH^+. We have previously discussed simple models that quantify the branching ratio between MH^+ and MCH_3^+ production in the reactions of atomic metal ions and methane.[54] These indicate that for a statistically behaved intermediate, a branching ratio between 4 and 20 can be expected, depending on the molecular constants of the products.[54] A branching ratio of >20 implies a direct reaction and in the impulsive limit can be as high as 90.[54] Thus, the reaction of $Fe(CO)^+$ with methane at these higher energies, like that of $Fe^+(^4F)$, probably occurs via a direct mechanism in which there are no long-lived, statistically-behaved intermediates. Because the cross section for reaction 7 is below our detectability limit for the $L = H_2O$ system, a branching ratio for FeH^+ and $FeCH_3^+$ cannot be explicitly obtained for $Fe(H_2O)^+$. A lower limit to this branching ratio is >18, also suggesting a direct mechanism.

Table 4. Branching Ratios, Reactions with Ethane

species	total cross section of activation (Å^2)	branching ratio (C−H/C−C)
$Fe^+(^6D)$	0.7[a]	0.4[a]
$Fe^+(^4F)$	7.1[a]	1.0[a]
$Fe(CO)^+(^4\Sigma^-)$	1.9[b]	1.3[b]
$Fe(H_2O)^+(^6A_1)$	2.1[b]	3.2[b]

[a] Reference 11. [b] This work.

The branching ratios of C−H to C−C bond activation for $Fe^+(^6D,^4F)$ and FeL^+ with ethane (calculated using the sums of the $LFeR^+$ and FeR^+ cross sections) are listed in Table 4. These results show that changing the ligation of the metal affects not only the reactivity of the metal center but also its *selectivity*. Although the probability of reaction (total cross section for σ-bond activation) is essentially the same for both L = CO and H_2O, there is a strong preference for C−H bond activation over C−C bond activation in the case of $Fe(H_2O)^+(^6A_1)$. Another indication of this strong preference is that the dehydrogenation reactions, processes 21 and 22, are observed only in the H_2O system. $Fe^+(^6D)$, however, shows a strong preference for C−C bond activation, and the Fe^+ and $Fe(CO)^+$ quartet states have a C−H/C−C branching ratio near unity.

The rationale for these observations is not immediately clear, but presumably involves a balance between thermodynamic, electronic, and steric effects. Certainly, $Fe^+(^6D)$, which reacts impulsively,[11] prefers C−C bond activation because this is the thermodynamically favorable channel. The more reactive $Fe^+(^4F)$ state balances this thermodynamic preference with the number of C−H vs C−C bonds in ethane. The more accessible and abundant C−H bonds then become equivalent bond activation targets. $Fe(CO)^+(^4\Sigma^-)$ acts much like the ^4F state with a reduced overall reaction probability due to the electronic considerations discussed above. For FeH_2O^+, the destabilization of the Fe^+-CH_3 interaction by the π-donating H_2O ligand makes C−C bond activation less favored thermodynamically than in the previously mentioned cases, and hence the efficiency of this channel is suppressed.

Acknowledgment. This work is supported by the National Science Foundation, Grant No. CHE-350412.

JA9601043

(53) Holthausen, M. C.; Fiedler, A.; Schwarz, H.; Koch, W. *J. Phys. Chem.* **1996**, *100*, 6236.

(54) Aristov, N.; Armentrout, P. B. *J. Phys. Chem.* **1987**, *91*, 6178.